Muon spin relaxation in some multiferroic fluorides

Anton Potočnik,* Andrej Zorko, Denis Arčon, Evgenij Goreshnik, and Boris Žemva
"Jožef Stefan" Institute, Jamova 39, 1000 Ljubljana, Slovenia

Robert Blinc and Pavel Cevc
"Jožef Stefan" Institute, Jamova 39, 1000 Ljubljana, Slovenia
and "J. Stefan" International Postgraduate School, 1000 Ljubljana, Slovenia

Zvonko Trontelj and Zvonko Jagličić
Institute of Mathematics, Physics and Mechanics, Jadranska 19, 1000 Ljubljana, Slovenia

James F. Scott
Department of Earth Sciences, University of Cambridge, Cambridge CB2 3EQ, England
(Received 23 February 2010; revised manuscript received 11 May 2010; published 15 June 2010)

Muon spin relaxation (μSR) has been employed to investigate the local magnetic properties of multiferroics $K_3Fe_5F_{15}$, $K_3Cr_2Fe_3F_{15}$, and $K_3Cu_3Fe_2F_{15}$. In all investigated systems μSR revealed a linear F-μ^+-F "hydrogenlike" bonded complex with the F-F distance of 2.43(2) Å in the paramagnetic phase. Two consecutive magnetic transitions were found in all systems, in agreement with the magnetic susceptibility measurements. Whereas in the paramagnetic phase the local magnetic fields at muon sites are about 20 G, they strongly increase below the Néel temperature T_N and reach values of several kilogauss. The μSR results further suggest that the system is inhomogeneous below T_N with magnetically ordered clusters being embedded into a disordered matrix. This scenario is endorsed by our electron paramagnetic resonance results.

DOI: 10.1103/PhysRevB.81.214420 PACS number(s): 75.80.+q, 76.75.+i, 75.50.Lk

I. INTRODUCTION

Coexistence of ferromagnetism (FM) or antiferromagnetism (AFM) with ferroelectricity and/or ferroelasticity is a characteristic property of multiferroic systems. Coupling between the spontaneous magnetization, the electric polarization, and the spontaneous stress promises a vast number of new applications,[1,2] in the sensor industry, spintronics, and new memory devices.[3,4] The quest for finding robust room-temperature ferromagnetic ferroelectrics with a large macroscopic polarization, therefore, represents a major challenge. The vast majority of all-known ferroelectrics, magnetoelectrics, and multiferroics are oxides[5] for which the basic, atomic-level, requirements for the coexistence of ferroelectricity and magnetism in a single phase are mutually exclusive.[5–7] The drawback of the majority of these systems is that the linear coupling coefficient between the magnetization and the polarization is relatively small and that the transitions occur far below room temperature. Therefore, new families which would exhibit alternative ferroelectric mechanisms that are compatible with magnetic ordering are worthwhile investigating.

The specific reason for the investigation of fluoride multiferroics where the above restrictions do not apply, is to check whether room-temperature systems with a large coupling exist. $K_3Fe_5F_{15}$, $K_3Cr_2Fe_3F_{15}$, and $K_3Cu_3Fe_2F_{15}$ are members of a fluoride-based family of multiferroics[8] with many potential applications in which magnetoelectric coupling has been discovered.[9–12] $K_3Fe_5F_{15}$, in particular, is magnetoelectric with a ferroelectric transition at T_c=490 K and a magnetic transition at T_N=125 K. The dielectric and ferroelectric behavior of $K_3Cr_2Fe_3F_{15}$ and $K_3Cu_3Fe_2F_{15}$ is still being investigated and ferroelasticity seems to be present. In the paraelectric phase they all belong to the $P4/mbm$ space group while in the ferroelectric phase the $Pba2$ space group is realized. There are 2 f.u. per unit cell. Their tunnel structure (Fig. 1) consists of a framework of corner-sharing (Fe,Cr,Cu)F_6 octahedra. Electrical neutrality requires four Fe^{3+} ions and six Fe^{2+} ions in the unit cell of $K_3Fe_5F_{15}$. In $K_3Cr_2Fe_3F_{15}$ the Fe^{2+} ions are supposed to be in an effective high-spin state (S_{eff}=1) whereas they are in the Fe^{3+} state (S=5/2) in $K_3Cu_3Fe_2F_{15}$. According to bulk susceptibility measurements, all systems exhibit at least two magnetic phase transitions.[10–12]

The local magnetic structure of the above-mentioned fluorides is still not clear. Here we investigate this issue from a local insight by means of the muon spin relaxation (μSR) technique. We compare the obtained results with bulk mag-

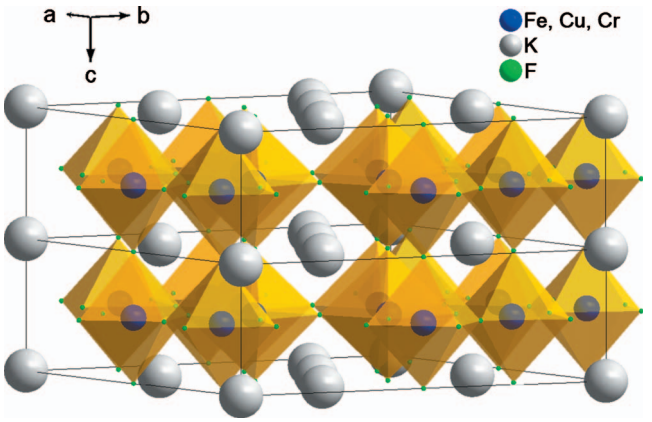

FIG. 1. (Color) Crystal structure of $K_3(Fe,Cr,Cu)Fe_2F_{15}$. The unit cells are marked by the black line.

netic susceptibility [superconducting quantum interference device (SQUID)] and electron paramagnetic resonance (EPR) results. The specific aim of our study is to determine local magnetic fields above and below the magnetic transition as well as to check whether these fluorides are magnetically homogeneous or intrinsically inhomogeneous systems. We, as well, wanted to determine the position of the implanted muons in the presumably formed F-μ^+-F "hydrogenlike" bond.

II. EXPERIMENTAL DETAILS

The details of the sample synthesis were published elsewhere.[10] The μSR measurements were performed on the μSR general purpose system facility at the Paul Scherer Institute, Switzerland. The bulk dc magnetic measurements were performed on the Quantum Design MPMS-XL-5 SQUID magnetometer in the external field of 1 kOe between 2 and 400 K. The X-band continuous wave EPR measurements were carried out on the commercial Bruker E580 spectrometer using a TE102 dual cavity and an Oxford cryogenics continuous flow E900 cryostat. The temperature stability was better than 0.1 K over the entire temperature range. For each compound all measurements were performed on the same batch of samples.

III. RESULTS AND DISCUSSION

A. Bulk magnetic susceptibility

Magnetic susceptibility measurements (magnetization divided by the applied magnetic field) are summarized in Fig. 2. They are performed on newly synthesized samples and are similar but not identical to the results previously published.[10–12] In $K_3Fe_5F_{15}$ (Ref. 10) a sharp first-order antiferromagnetic transition takes place at T_N=125 K. Simultaneously, a splitting between field-cooled (FC) and zero-field-cooled (ZFC) susceptibility data occurs, which suggests that the system is a magnetic relaxor [Fig. 2(a)]. Another first-order transition is seen around 80 K. In addition, a narrow magnetic hysteresis loop was reported before[10] below T_N=125 K and rationalized as a change in the AFM structure into a weakly ferromagnetic one due to spin canting.

In $K_3Cr_2Fe_3F_{15}$ [Fig. 2(b)] two magnetic transitions are also found, one at T_N=37 K and another around 17 K. The splitting between FC and ZFC susceptibilities is again observed below T_N. A narrow hysteresis loop was found before and observed frequency dispersion further suggested a magnetic relaxor system.[11]

In $K_3Cu_3Fe_2F_{15}$, on the other hand, there is no splitting between the FC and ZFC static magnetic susceptibility data and no frequency dispersion was observed[12] in the ac magnetic susceptibility. In contrast to the above two systems, $K_3Cu_3Fe_2F_{15}$ apparently does not seem to be a relaxor or a weak ferromagnet. However, all systems exhibit at least two anomalies in the magnetic susceptibility, implying multiple magnetic phase transitions. Clear anomalies in the magnetic susceptibility of $K_3Cu_3Fe_2F_{15}$ are seen at T_N=88 K and 40 K [Fig. 2(c)].

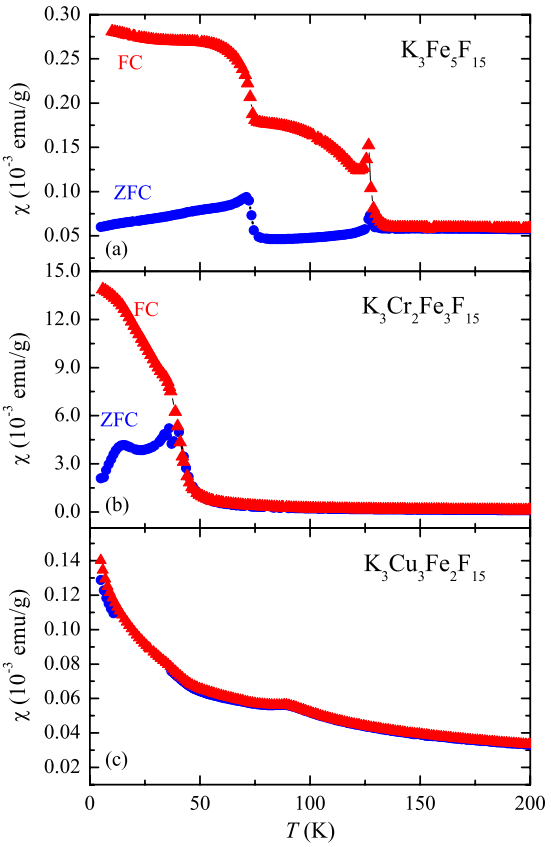

FIG. 2. (Color online) FC and ZFC SQUID measurements of (a) $K_3Fe_5F_{15}$, (b) $K_3Cr_2Fe_3F_{15}$, and (c) $K_3Cu_3Fe_2F_{15}$.

B. Muon spin relaxation (μSR)

μSR can locally detect both static magnetic fields with extreme sensitivity as well as fluctuating fields in a broad range of frequencies.[13] Positive muons are initially almost 100% polarized along the beam direction. Magnetic coupling of the muon with local magnetic fields causes a precession of the muon polarization, which decays due to a distribution of the magnetic fields. When the fields are static, statistically 1/3 of the muons are nonprecessing because their polarization is parallel to the local fields. This is the origin of the characteristic 1/3-tail in the zero-field powder μSR. It is regarded as one of the firmest evidences of a magnetic state with static moments, either ordered or disordered.[13] The shape of the remaining relaxing 2/3 component of the polarization reflects the distribution of the static local fields at the muon site. For a long-range ordered state several oscillations are regularly observed. These become more damped for spatially inhomogeneous field distributions. If the static fields are randomly distributed a single dip remains and a characteristic Kubo-Toyabe relaxation curve is observed.[13]

At high temperatures we observed in all three samples an irregularly oscillating μ^+ asymmetry [Fig. 3(a)]. Such a signal cannot be explained either with static local fields originating from ordered electronic moments nor with the Kubo-Toyabe relaxation corresponding to randomly distributed frozen electronic or nuclear fields.[14] Actually, in samples containing fluorine a specific relaxation was observed in the

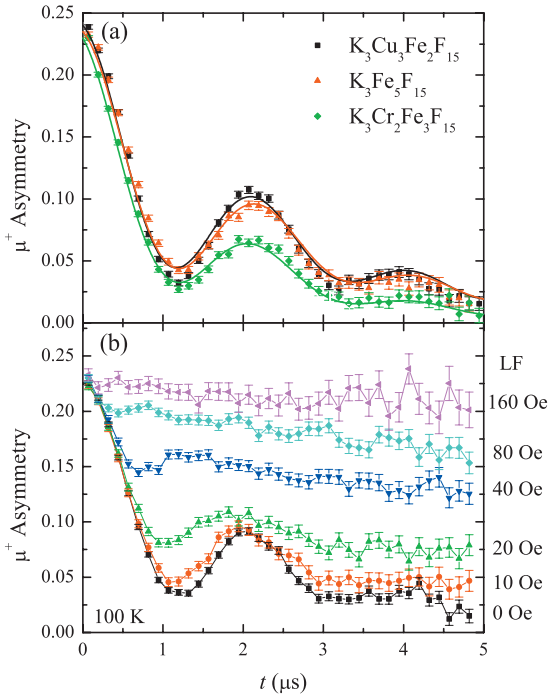

FIG. 3. (Color) (a) Irregular oscillations of the μ^+ asymmetry at zero magnetic field in the paramagnetic phase due to the entangled linear F-μ^+-F complex with the F-F length of $2r$=2.43(2) Å, which is the same for all three investigated fluorides. (b) Field-decoupling experiment in longitudinal field (LF) in $K_3Cu_3Fe_2F_{15}$.

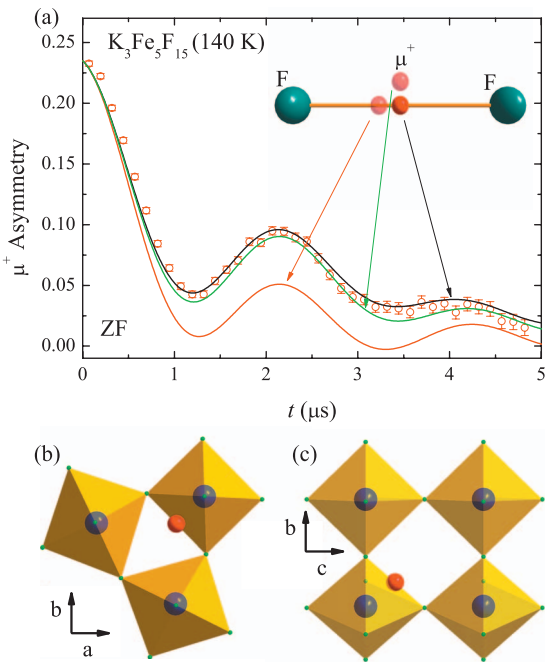

FIG. 4. (Color) (a) Simulation of the μ^+ asymmetry decay for different muon positions between the two F^- ions gives the best agreement for the central position of the muon. Free parameters in the simulation are the F-F distance [$2r$=2.43(2) Å] and the μ^+ relaxation rate (λ=0.31 MHz); two possible muon positions inside the structure marked with a red ball (b) in a triangular environment and (c) in a square environment.

past.[15–18] It results from an entanglement of the muon magnetic moment and fluorine nuclear moments when muons are bound to nearby fluorine ions.

In order to determine the muon position in the structure more precisely we have simulated several entangled states. The Hamiltonian for muon and fluorine nuclei interacting through the dipolar interaction is written as

$$\mathcal{H} = \sum_{i>j} \frac{\mu_0 \gamma_i \gamma_j}{4\pi |\boldsymbol{r}_{ij}^3|} [\boldsymbol{S}_i \cdot \boldsymbol{S}_j - 3(\boldsymbol{S}_i \cdot \hat{\boldsymbol{r}}_{ij})(\boldsymbol{S}_j \cdot \hat{\boldsymbol{r}}_{ij})], \tag{1}$$

where γ_i and γ_j are gyromagnetic ratios for either the muon ($\gamma_\mu = 2\pi \times 135.5$ MHz/T) or fluorine ($\gamma_F = 2\pi \times 40.5$ MHz/T), $\boldsymbol{S}_i$ is the muon or fluorine spin vector, $\boldsymbol{r}_{ij}$ is the vector connecting the spins $\boldsymbol{S}_i$ and $\boldsymbol{S}_j$, and $\hat{\boldsymbol{r}}_{ij} = \boldsymbol{r}_{ij}/|\boldsymbol{r}_{ij}|$. The μSR experiment measures the polarization of the muon ensemble $P_z(t)$ along the initial muon direction, z. It is for the powder samples given by[19]

$$P_z^0(t) = \frac{1}{N} \left\langle \sum_{m,n} |\langle m|\sigma_q|n\rangle|^2 \exp(i\omega_{m,n} t) \right\rangle_q . \tag{2}$$

Here N is the number of spins, $|m\rangle$ and $|n\rangle$ are eigenstates of the total Hamiltonian $\mathcal{H}$, σ_q is the Pauli spin matrix corresponding to the direction q, and $\langle\ \rangle_q$ represents the powder average over all directions. The muon polarization is usually calculated using the following expression:[16]

$$P_z(t) = \exp[-(\lambda t)^\beta] P_z^0(t), \tag{3}$$

where λ is the relaxation rate and β the stretch exponent. In our case we fix β=1, because this parameter did not improve the quality of the fit noticeably. The only free parameters are thus the spatial coordinates of the ions with respect to the muon and λ. As it can be seen from Fig. 4(a) the best fit with the experimental μ^+ asymmetry is obtained for a linear symmetric F-μ^+-F bond. The asymmetric location of the μ^+ in the bond gives a significantly worse fit. The same is true for a symmetric nonlinear F-μ^+-F bond where the muon is located out of the F-F direction. The two possible positions of the muon in the structure, which can form a linear F-μ^+-F complex and are far away from the K^+ cations are depicted in Figs. 4(b) and 4(c). The cases of the muons sitting in the center of a triangle and a square fluorine environment (which might be inspected from the crystal structure) resulted in much worse fits.

For all three samples the μ^+ asymmetry decay is best fitted with a linear F-μ^+-F complex[15] with a fluorine-to-fluorine distance of 2.43(2) Å. Thus it seems that muons locally distort the crystal structure since the calculated F-F distance in the F-μ^+-F complex is significantly below typical F-F distances in the samples (2.7–2.9 Å). The average magnetic field at the muon site is $B_{F\mu F} \sim 21$ G, as estimated from our fits.

To confirm the static nature of the local field in the entangled state, we show in Fig. 3(b) a field-decoupling experiment, where the external magnetic field H_L is applied in the

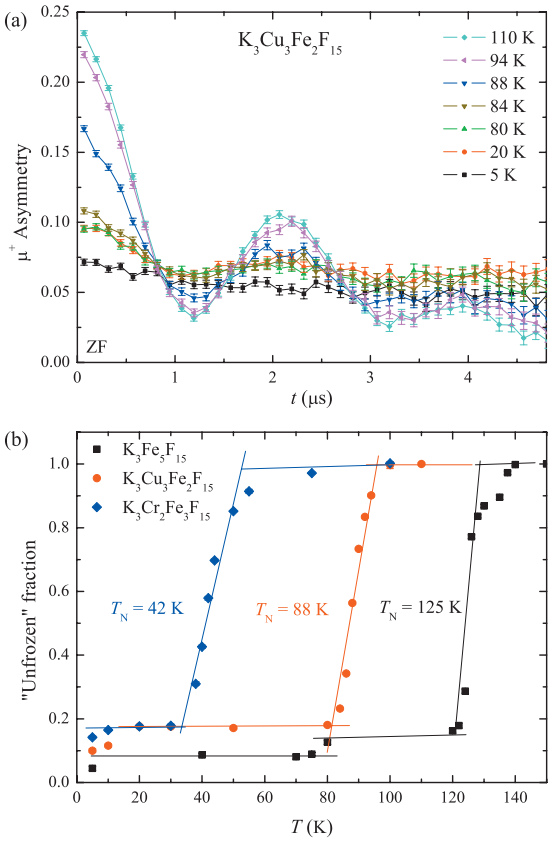

FIG. 5. (Color) (a) Temperature dependence of the μ^+ asymmetry decay in $K_3Cu_3Fe_2F_{15}$. (b) Temperature dependence of the F-μ^+-F relaxation amplitude (i.e., "unfrozen" fraction) of all three samples. The obtained Néel temperatures are in good agreement with those determined by the SQUID measurements.

longitudinal direction of the initial muon polarization, z. When H_L becomes on the order of the internal static field it helps aligning the total field at the muon site along the z direction, effectively decreasing the muon depolarization. On the other hand, much higher fields are needed to affect the muon depolarization if the decay is due to fluctuating local fields.[13] It can be seen in Fig. 3(b) that the longitudinal field of H_L=20 Oe already changes the decay curve, which confirms the static nature of local fields.

Below T_N the local field at the muon site becomes much larger than the F-μ^+-F dipolar fields. This leads to high-frequency oscillations of the muon polarization at early times and the disappearance of F-μ^+-F oscillations [Fig. 5(a)]. Relaxation curves reveal that the characteristic F-μ^+-F signal does not disappear at once below T_N. By following the amplitude of the relaxation curve we obtain the temperature dependence of the unfrozen fraction of the sample [Fig. 5(b)], where static electronic magnetic fields are not yet present. We note that the signal from frozen parts of the sample effectively contributes to the 1/3 tail, which causes the increase in the μ^+ asymmetry at longer times. The temperature dependence of the unfrozen fraction reveals (i) that the transition below T_N is gradual, i.e., parts with frozen and unfrozen electronic fields coexist in a relatively broad temperature interval, and (ii) that the majority of the electronic spins forms statistically ordered magnetic clusters. The μ^+

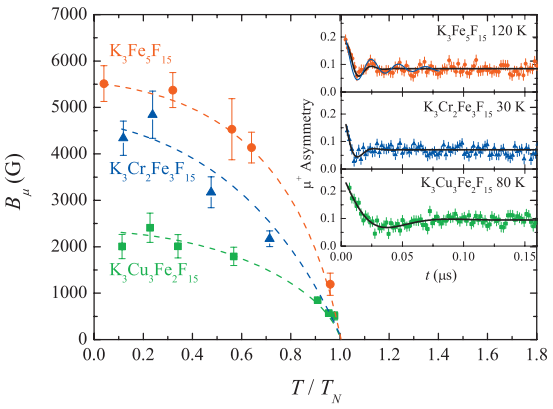

FIG. 6. (Color) Normalized temperature dependence of the local magnetic field below the magnetic phase transitions in $K_3Fe_5F_{15}$ (red circles, T_N=125 K), $K_3Cr_2Fe_3F_{15}$ (blue triangles, T_N=42 K), and $K_3Cu_3Fe_2F_{15}$ (green squares, T_N=88 K). Inset: high-frequency μ^+ asymmetry oscillations in magnetically ordered state just below T_N. Black lines represent damped cosine function fits [Eq. (4)] and the blue line in $K_3Fe_5F_{15}$ inset represents a Bessel function fit [Eq. (5)].

asymmetry with oscillations characteristic for the F-μ^+-F complex that remains present far below T_N (typically around 10%) is due to muons stopping in "nonordered" environments or in minor impurity phases of the sample. We note that the transition temperatures determined from μSR agree well with the bulk susceptibility measurements.

At temperatures below the magnetic phase transitions high-frequency oscillations of the μ^+ asymmetry [inset to Fig. 6(b)] allow us to follow the development of the local magnetic fields. The oscillations were fitted with the simplest possible model—a damped cosine function [Fig. 6(b)]

$$P_z(t) = A\,\exp(-\lambda t)\cos(2\pi\nu_\mu t + \Phi) + B_g, \qquad (4)$$

where A is the oscillation amplitude, λ the relaxation rate, ν_0 the oscillation frequency, Φ the oscillation phase, and B_g a constant background value originating from the 1/3 tail. The temperature dependence of the local magnetic field at the muon site below T_N calculated from $\nu_\mu = \gamma_\mu B_\mu$ can be seen in Fig. 6. The decay rate and saturated local magnetic fields for all three investigated substances are summarized in Table I. The local fields around the F sites in the ordered phase are on the order of several kilogauss. As expected, this is much less

TABLE I. Summary of extrapolated local magnetic fields at 0 K and the decay times at temperatures just below T_N for the corresponding samples. Parameters were obtained by fitting the μ^+ asymmetry oscillations in the magnetically ordered state (inset to Fig. 6) with a damped cosine function.

Sample	λ (MHz)	B_μ (G)
$K_3Fe_5F_{15}$	170 ± 80	5500 ± 500
$K_3Cr_2Fe_3F_{15}$	140 ± 40	4500 ± 1000
$K_3Cu_3Fe_2F_{15}$	60 ± 30	2500 ± 400

than at the Fe^{3+} sites where the local fields in the ordered phase are ~500 kG as determined from Mössbauer data.[11]

The required relaxation in our model for the frozen state is unexpectedly strong, i.e., on the order of 100 MHz (see Table I). It is unlikely that this relaxation is dynamic because (i) our fits do not imply any critical behavior near T_N, (ii) the 1/3 tail does not show any appreciable spin-lattice relaxation, and (iii) the Mössbauer spectra in the case of $K_3Fe_5F_{15}$ do not show dynamic effects as the intensity distribution of the six magnetic lines corresponds to the static case.[10] This observation then leads us to the conclusion that static local fields are inhomogeneous, possibly originating from spin clusters, typical for the spin-glass state. They may even come from an incommensurately distributed local fields. The latter seems particularly probable for $K_3Fe_5F_{15}$ where several oscillations are seen at early times (inset to Fig. 6). In case of an incommensurate magnetic structure the oscillations can in the first approximation be described by[13]

$$P_z^i(t) = A\left[\frac{2}{3}J_0(\gamma_\mu B_\mu t)\exp(-\lambda_l t) + \frac{1}{3}\exp(-\lambda_t t)\right] + B_g, \tag{5}$$

where J_0 is a Bessel function, λ_l is the longitudinal relaxation rate, and λ_t is the transverse relaxation rate. For $K_3Fe_5F_{15}$ (inset to Fig. 6), the early oscillations can be merely equally well described by an incommensurate structure [blue fit, $\lambda_l = 16.8(2)$ MHz and $\lambda_t = 1.8(2)$ MHz] or by the presence of damping [Eq. (4)]. In the following (Table I) we decided for the sake of simplicity to use the strongly damped cosine fit [Eq. (4)]. The muon asymmetry in the $K_3Cr_2Fe_3F_{15}$ and $K_3Cu_3Fe_2F_{15}$ samples, on the other hand, resembles the Kubo-Toyabe relaxation function (inset to Fig. 6), pointing toward a spin cluster state.

C. EPR

The EPR spectra of $K_3Fe_5F_{15}$ are shown for comparison in Fig. 7 together with the temperature dependence of the EPR intensity (χ_{EPR}), linewidth (ΔH), and g factor. It should be pointed out, as shown below, that the EPR spectrum mainly reflects the behavior of the disordered part of the sample, no signal from the ordered part is observed at low temperature. Above T_N, in the paramagnetic phase, the EPR intensity decreases with decreasing temperature as expected for an AFM system when AFM correlations set in. However, it does not completely vanish below T_N. In fact, it slowly drops for nearly one half and remains constant when passing the first magnetic phase transition ($T_{N1}=125$ K). Below the second magnetic phase transition ($T_{N2}=80$ K as evidenced by susceptibility and μSR) the EPR intensity begins to decrease again, thus showing the presence of two AFM transitions as expected. With decreasing temperatures the intensity vanishes below 15 K, indicating that all iron moments order. This scenario is endorsed by the peak in the EPR linewidth at 15 K. The g factor slowly changes with decreasing temperature down to T_{N2}. Below T_{N2} it starts to increase more pronouncedly, indicating that the local AFM field is opposite to the applied external field. At ~40 K it suddenly drops, demonstrating the presence of spin canting leading to a weakly ferromagnetic phase.

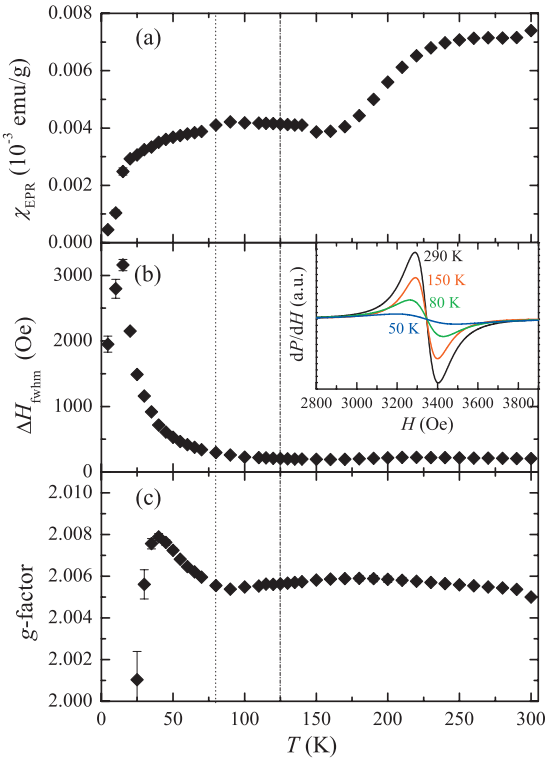

FIG. 7. (Color) (a) Temperature dependence of the $K_3Fe_5F_{15}$ EPR line intensity, (b) the EPR linewidth, and (c) the g factor. Dotted and dashed-dotted lines indicate magnetic transitions at 80 K (T_{N2}) and 125 K (T_{N1}), respectively. Inset: EPR spectra of $K_3Fe_5F_{15}$.

We observed neither antiferromagnetic nor ferromagnetic resonance lines in the X-band, which should occur at far infrared frequencies. The EPR signal below T_{N1} simply continuously evolves from the paramagnetic phase and thus seems to belong to the disordered parts of the sample. This is further supported by the calibrated intensity of the EPR line. To summarize, previously obtained Mössbauer spectra[10] show that the magnetic field at Fe site is on the order of 500 kG below 125 K, whereas the fields extracted from the EPR data are on the order of 200 G below 50 K and increase up to 3000 G around 10 K. This discrepancy shows that the structure of the system is strongly inhomogeneous. The EPR line as we see it arises from the disordered parts of the system, where the magnetic fields are smaller and not from the bulk where there are hundred and more times stronger. All this observations indicate that we deal below T_{N1} with a two-component percolation-type system. There are ordered parts with a large FM- or AFM-type internal field which vanishes above T_{N1}, as well as paramagneticlike regions which stay disordered. The fraction of the disordered regions is according to the μSR as well as EPR data of the order of 10% below T_{N1}, which agrees also with the Mössbauer data.[10] This cannot be accounted for by impurities. It thus seems that the disordered clusters are intrinsic and a characteristic property of the systems. The situation is similar in $K_3Cr_2Fe_3F_{15}$ (Ref. 12) and $K_3Cu_3Fe_2F_{15}$.[11]

IV. CONCLUSIONS

μSR, magnetic susceptibility and EPR measurements all show the occurrence of at least two magnetic phase transitions in the three investigated samples. In μSR a particular relaxation function was observed in the paramagnetic phase which allowed to determine the existence of a symmetric F-μ^+-F hydrogenlike bond with the F-F distance of 2.43(2) Å. The local field at the muon site is here ~20 G. In the magnetically ordered state the muon relaxation revealed the temperature dependence of the local magnetic fields. The saturating fields at $T \rightarrow 0$ are 5500 G, 4500 G, and 2500 G for $K_3Fe_5F_{15}$, $K_3Cr_2Fe_3F_{15}$, and $K_3Cu_3Fe_2F_{15}$, respectively. The observed fast μ^+ relaxation indicates highly inhomogeneous magnetic fields in the ordered state. This may be a spin glass (magnetic relaxorlike) state or an incommensurate magnetically ordered state. The EPR spectra observed below T_N arise from the disordered regions in the sample and indicate a magnetic percolation-type behavior below T_N. Magnetic nanoclusters seem to be embedded in a disordered matrix.

ACKNOWLEDGMENTS

We thank A. Amato and H. Luetkens for technical assistance with μSR measurements. This research project was partially supported by the European Commission under the 7th Framework Programme through the "Research Infrastructures" action of the "Capacities" Programme, Contracts No. CP-CSA_INFRA-2008-1.1.1 and No. 226507-NMI3, and the 7th Framework Multiceral project. This work was partially performed and financed as a part of EN→FIST Centre of Excellence, Dunajska 156, SI-1000 Ljubljana, Slovenia.

*anton.potocnik@ijs.si

[1] M. Fiebig, J. Phys. D: Appl. Phys. **38**, R123 (2005).
[2] W. Eerenstein, N. D. Mathur, and J. F. Scott, Nature (London) **442**, 759 (2006).
[3] M. Gajek, M. Bibes, S. Fusil, K. Bouzehouane, J. Fontcuberta, A. Barthélémy, and A. Fert, Nature Mater. **6**, 296 (2007).
[4] R. Ramesh and N. A. Spaldin, Nature Mater. **6**, 21 (2007).
[5] S.-W. Cheong and M. Mostovoy, Nature Mater. **6**, 13 (2007).
[6] R. E. Cohen, Nature (London) **358**, 136 (1992).
[7] N. A. Hill, J. Phys. Chem. B **104**, 6694 (2000).
[8] S. C. Abrahams, Acta Crystallogr., Sect. B: Struct. Sci. **45**, 228 (1989).
[9] J. Ravez, S. C. Abrahams, and R. de Pape, J. Appl. Phys. **65**, 3987 (1989).
[10] R. Blinc, G. Tavčar, B. Žemva, D. Hanžel, P. Cevc, C. Filipič, A. Levstik, Z. Jagličić, Z. Trontelj, N. S. Dalal, V. Ramachandran, S. Nellutla, and J. F. Scott, J. Appl. Phys. **103**, 074114 (2008).
[11] R. Blinc, G. Tavčar, B. Žemva, E. Goreshnik, D. Hanžel, P. Cevc, A. Potočnik, V. Laguta, Z. Trontelj, Z. Jagličić, and J. F. Scott, J. Appl. Phys. **106**, 023924 (2009).
[12] R. Blinc, P. Cevc, A. Potočnik, B. Žemva, E. Goreshnik, D. Hanžel, A. Gregorovič, Z. Trontelj, Z. Jagličić, V. Laguta, M. Perovič, N. S. Dalal, and J. F. Scott, J. Appl. Phys. **107**, 043511 (2010).
[13] *Muon Science: Muons in Physics, Chemistry, and Materials*, edited by S. L. Lee, S. H. Kilcoyne, and R. Cywinski (Taylor & Francis, Abingdon, 1999).
[14] R. Kubo, Hyperfine Interact. **8**, 731 (1981).
[15] M. Celio and P. F. Meier, Phys. Rev. B **27**, 1908 (1983).
[16] J. H. Brewer, S. R. Kreitzman, D. R. Noakes, E. J. Ansaldo, D. R. Harshman, and R. Keitel, Phys. Rev. B **33**, 7813 (1986).
[17] T. Lancaster, S. J. Blundell, P. J. Baker, W. Hayes, S. R. Giblin, S. E. McLain, F. L. Pratt, Z. Salman, E. A. Jacobs, J. F. C. Turner, and T. Barnes, Phys. Rev. B **75**, 220408(R) (2007).
[18] T. Lancaster, S. J. Blundell, P. J. Baker, M. L. Brooks, W. Hayes, F. L. Pratt, J. L. Manson, M. M. Conner, and J. A. Schlueter, Phys. Rev. Lett. **99**, 267601 (2007).
[19] E. Roduner and H. Fischer, Chem. Phys. **54**, 261 (1981).